STRESS CORROSION TESTING WITH PRE-CRACKED SPECIMENS: INFLUENCE OF THE PRE-CRACKING PROCEDURE

J. Toribio* and A.M. Lancha†

The influence of the pre-cracking procedure on the stress corrosion behaviour of pre-cracked specimens is analyzed. The very important role is demonstrated of compressive residual stresses —generated in the vicinity of the crack tip during fatigue cracking of the samples— in SCC processes. These effects were included in ISO 7539-6 standard, which recommends that pre-cracking should be completed below the expected SCC threshold K_{ISCC}, if possible. However, this requirement is not clearly objective, since the threshold has no intrinsic character but is affected by the pre-cracking procedure. The role of residual stresses in both anodic dissolution and hydrogen assisted cracking phenomena is discussed. Guidelines for improving present standards for stress corrosion testing are also provided.

INTRODUCTION

In recent years, slow strain rate tests (SSRT) have become widely used and accepted for stress corrosion cracking evaluations by research centres and industries, since strain rate plays an important mechanistic role in stress corrosion cracking (SCC), according to Parkins (1). However, some limitations of this technique —concerning strain rate and potential dependence— have been discussed by Beavers and Koch (2).

In the matter of standardization, three major efforts are reported by Kane and Wilhelm (3): ASTM task Group G-1, NACE Committee T-1, and ISO. The first two are now working in drafts of standards for SSRT. The only consensus standard currently fully developed has been provided by ISO, as part of a seven-part document entitled: "Stress Corrosion Testing" (ISO 7539), whose section 7 (ISO 7539-7) is entitled: "Slow strain rate testing" (4).

* Department of Materials Science, University of La Coruña, E.T.S.I. Caminos, Campus de Elviña, 15192 La Coruña, Spain.
† CIEMAT, Ciudad Universitaria, 28040 Madrid, Spain.

Although a variety of specimens (initially plain, notched and pre-cracked) can be used (cf. ISO 7539-7), a specific part of the standard is devoted to pre-cracked samples: ISO 7539-6: "Preparation and use of pre-cracked specimens" (5). These specimens present clear advantages since they are quite realistic, and the effect of the environment is localized in the vicinity of the notch tip, apart from the fact that fracture mechanics techniques are applicable.

However, there is an additional variable —not sought— which produces spurious effects on results: compressive residual stresses in the vicinity of the crack tip, generated during fatigue pre-cracking of the samples. This effect was reported previously by Lancha and Elices (6) and Judy *et al.* (7). Fatigue pre-cracking of specimens requires a great deal of care to ensure that experimental results are not influenced by compressive residual plastic regions, thereby producing a negative consequence in the form of unacceptable experimental scatter if the fatigue pre-cracking programme is not carefully controlled.

This fact was taken into account in the ISO 7539-6 standard (5), which gives recommendations concerning the maximum stress intensity factor during the last step of fatigue pre-cracking. The role of residual stresses in both localized anodic dissolution and hydrogen assisted cracking is discussed in later sections. A major issue to be addressed is the actual meaning of thresholds in environmentally assisted cracking processes. Guidelines for improving present standards for stress corrosion testing are also provided.

SLOW STRAIN RATE TESTS

Experimental Procedure

The experiments were performed on a commercial eutectoid pearlitic steel, supplied in bar form of 12mm diameter, whose chemical composition and mechanical properties appear in Table 1. The specimens were transversely pre-cracked rods, in which a transverse pre-crack was produced by axial fatigue in air (Figure 1). The crack depth was the same for all specimens: a = 4.0±0.2 mm. Samples were coated with an insulating lacquer except for a band about 1 mm wide on each side of the pre-crack, to restrict the environmental attack to the crack tip.

TABLE 1 – Chemical composition (wt %) and mechanical properties of the steel

C	Mn	Si	P	S	E (GPa)	σ_Y (MPa)	UTS (MPa)	K_{IC} (MPa $m^{1/2}$)	K_{1C} (MPa $m^{1/2}$)
0.74	0.70	0.20	0.016	0.023	195	725	1300	53	65

For these samples of high strength steel, it has been proved by Elices (8) that Linear Elastic Fracture Mechanics (LEFM) is applicable, since the plane strain condition is reached at most points of the crack. In this case the fracture toughness

of the material (K_{IC} in Table 1) can be measured by using an expression for the maximum stress intensity factor at the deepest point of the crack, calculated by Astiz (9) by the Finite Element Method (FEM) combined with a Virtual Crack Extension technique. The value K_{1C} in Table 1 represents the critical stress intensity factor for the prismatic three-point bend specimens used in the constant strain tests (CST) described in following sections. They are machined from the commercial 12 mm bar and are not thick enough to reach the plane strain situation at any point of the crack. The experimental procedure for measuring K_{1C} in these samples was reported by Lancha (10).

Samples were subjected to slow strain rate testing (1–3). The crosshead speed was 8.3×10^{-8} ms^{-1}, following previous experience. (Parkins *et al.* (11)). Macroscopic susceptibility to hydrogen was measured through the ratio of the failure load in hydrogen to that in air, as recommended by ISO Standard (3). In addition, a SEM fractographic analysis after fracture was performed. The aggressive environment was an aqueous solution of 1 g/l $Ca(OH)_2$ + 0.1 g/l NaCl (pH=12.5). All tests were carried out under potentiostatic control, covering a broad range from E = –1200 mV SCE to E = –100 mV SCE, so as to distinguish two different regimes of environmentally assisted cracking (EAC): a cathodic regime (below –900 mV SCE), in which the predominant mechanism is ***hydrogen assisted cracking*** (HAC), and an anodic regime (above –600 mV SCE), in which the main process is *localized anodic dissolution* (LAD).

Pre-cracking of the samples was carried out in the normal laboratory air environment. To evaluate the influence of the pre-cracking procedure, several types of samples were prepared by using different fatigue pre-cracking loads during the last step (just previous to the fracture test). Figure 2 shows the fatigue programmes used to induce different degrees of compressive residual stress at the crack tip. The maximum fatigue pre-cracking loads used during the last step were 0.28 K_{IC}, 0.45 K_{IC}, 0.60 K_{IC} and 0.80 K_{IC}.

Influence of the Pre-Cracking Procedure

For a typical cathodic regime (–1200 mV, HAC) the results are practically independent of pH, as shown in Figure 3. Susceptibility to HAC decreases as the maximum fatigue load increases, and this occurs for all values of K_{max}. Figure 4 shows the experimental results for a typical anodic regime (–400 mV, LAD), which depend on the pH. Susceptibility to LAD decreases as the maximum fatigue load increases. In addition, the aggressiveness of the environment rises as the pH of the solution becomes more acid.

These K_{max}-effects, due to the compressive residual stresses in the vicinity of the crack tip generated during pre-cracking, were considered in the ISO 7539-6 standard, which recommends that pre-cracking should be completed below the expected SCC threshold K_{ISCC}, if possible. However, this requirement is not clearly objective, since the threshold has no intrinsic character, but is affected by the pre-cracking procedure itself, as is demonstrated in the following section, devoted to constant strain tests. The consequence from the experimental viewpoint is an undesirable increase in the scatter of results when the maximum fatigue pre-cracking load is not properly controlled.

CONSTANT STRAIN TESTS

Experimental Procedure

Constant strain tests (CST) were carried out on three-point bend prismatic specimens of 3.85x7.70x100.00 mm, machined from the 12 mm diameter rod bars, with a starter notch in its central section, perpendicular to the bar axis. Cracking was produced by axial fatigue in air environment, previous to the CST. Samples were subjected to constant strain tests in a cell containing the same aqueous solution as that used in the SSRT (1 g/l $Ca(OH)_2$ plus 0.1 g/l NaCl, pH = 12.5). Two electrochemical potentials were used: E=–1200mV SCE (cathodic regime: hydrogen assisted cracking–HAC) and E=–600mV SCE (anodic regime: localized anodic dissolution–LAD).

Load was applied by means of a three point bend device with a distance between supports of 61.60 mm. Both the load on the sample and the crack length were measured during the test; the first through the load cell of the machine, and the second by standard optical methods. Strain was increased step by step to have different points of the curve crack growth rate vs. stress intensity factor. The latter was calculated from the crack length and the applied load by a standard expression. Each externally applied strain was maintained for 23 hours, which establishes a limit for the minimum detectable crack growth rate of 10^{-9} m/s.

Two types of samples were prepared by using different fatigue pre-cracking loads during the last step (just previous to the fracture test). The maximum stress intensity factors during fatigue pre-cracking were $K_{max} = 0.25\ K_{1C}$ and $0.50\ K_{1C}$, where K_{1C} means the critical stress intensity factor for the prismatic three point bend specimens used in the experimental programme (a value greater than the fracture toughness of the material K_{IC}, since the thickness was not enough to fulfil the plain strain condition requirements). This fact implies two unlike distributions of compressive residual stresses in the vicinity of the crack tip, and therefore two distinct degrees of delay for the environmentally assisted cracking process.

Influence of the Pre-Cracking Procedure

This section deals with the influence of the fatigue pre-cracking load on the threshold stress intensity factor for environmentally assisted cracking (K_{IEAC}, or in traditional form K_{ISCC} or K_{TH}), distinguishing between the thresholds for hydrogen assisted cracking (K_{IHAC}) and localized anodic dissolution (K_{ILAD}).

Results for E=–1200 mV SCE (cathodic regime: hydrogen assisted cracking–HAC) are plotted in Figure 5. For a maximum fatigue pre–cracking load $K_{max} = 0.25\ K_{1C}$, the threshold stress intensity factor for HAC is $K_{IHAC} = 0.35\ K_{1C}$. Below this value no crack propagation is observed. For higher levels of K_I there is a plateau ($da/dt = 1.5x10^{-7}$ m/s), then a sudden increase up to about 10^{-3} m/s, a slightly sloped section and finally the catastrophic fracture. For $K_{max} = 0.50K_{1C}$ the threshold for HAC is $K_{IHAC} = 0.58\ K_{1C}$. No plateau is observed for higher K_I, but a sudden increase to about 10^{-3} m/s. The threshold value shows important changes ($0.35\ K_{1C}$ against $0.58\ K_{1C}$) under cathodic regime, depending on the maximum stress intensity factor, K_{max}.

Results for E = –600 mV SCE (anodic regime: localized anodic dissolution-LAD) appear in Figure 6. For a maximum fatigue pre-cracking load $K_{max} = 0.25\ K_{1C}$ the threshold stress intensity factor for LAD is $K_{ILAD} = 0.75\ K_{1C}$. For higher values of K_I there is a pseudo-plateau ($da/dt \approx 5x10^{-3}$ m/s) up to $0.90\ K_{1C}$. When K_I exceeds this level, final fracture takes place under pure mechanical factors (K_I close to K_{1C}). For $K_{max} = 0.50\ K_{1C}$ the threshold for LAD is so high that even for $K_I = 0.95\ K_{1C}$ no propagation can be detected, which means that the environmental process is negligible in this case ($K_{ILAD} \approx 0.96\ K_{1C}$). Pre-cracking conditions are so relevant under anodic regime (LAD), that they even impede the environmentally assisted cracking when K_{max} is high enough, and thus no actual threshold can be detected.

DISCUSSION

The analysis of both HAC and LAD phenomena demonstrates the very important role of residual stresses in the vicinity of the crack tip. These residual stresses — compressive type— are generated near the crack tip during the fatigue pre-cracking procedure, and produce an extremely high *scatter* in experimental results if they are not carefully controlled during the test. As a consequence, the important variable Kmax should be included in the display of the SSRT and CST results, since it has been shown to be determinant in explaining the EAC behaviour of the material, according to Figures 3 to 6.

With regard to the concept of *stress intensity threshold in environmentally assisted cracking* (K_{IEAC}, K_{ISCC} or K_{TH}) it does not seem to have an intrinsic character, but depends on certain variables such as the maximum stress intensity level during the last step of fatigue pre-cracking, which strongly influences the threshold itself, as shown in Figure 7, where the threshold values for HAC (cathodic) and LAD (anodic) are plotted against the maximum stress intensity factor during fatigue pre-cracking (K_{max}). Values are divided by the critical stress intensity factor K_{1C}, and the rough tendencies are the following:

$$(K_{IHAC} / K_{1C}) = 0.12 + 0.92\ (K_{max} / K_{1C}) \quad (1)$$

$$(K_{ILAD} / K_{1C}) = 0.54 + 0.84\ (K_{max} / K_{1C}) \quad (2)$$

What is clear from Figure 7 and equations (1) and (2) is not only that the threshold value depends strongly on the maximum pre-cracking load, but also that the requirement of the ISO 7539-6 Standard is automatically reached, since the maximum stress intensity factor during final stage of fatigue pre-cracking (K_{max}) is *always* below the actual stress corrosion cracking threshold (K_{IEAC}). So the problem is precisely an experimental fact: K_{max} is automatically below K_{IEAC} because this threshold value is too high due to the presence of compressive residual stresses in the vicinity of the crack tip. The original idea of ISO 7539-6 is to reach a tensile stress level well above that of the final stage of pre-cracking when crack growth starts because the threshold is exceeded. However, this situation is impossible because residual stresses raise the threshold level. Such a coupling between material strength and threshold stress intensity factor has also been detected by Astafjev and Kasatkin (12).

A simple model to explain these effects due to compressive residual stresses in the vicinity of the crack tip is that of Rice (13), applied by Toribio *et al.*(14) to the modelling of hydrogen assisted cracking. Following this model, the size of the plastic zone after fatigue pre-cracking is:

$$\Delta\omega = (\pi/32)\ (K_{max} / \sigma_Y)^2 \qquad (3)$$

where σ_Y is the yield strength of the material, and pre-cracking stress distribution (that of the last peak of tensile load in fatigue) is recovered when the tensile load is applied in the fracture test, i.e., compressive residual stresses are deleted when the specimen is re-loaded up to the same tensile stress level as during fatigue.

Consequently for stress corrosion testing with pre-cracked specimens, SSRT in cathodic regime (HAC) should be performed at the minimum possible strain rate, to allow enough time for hydrogen to diffuse after recovering the initial tensile stress distribution. CST and threshold measurement are particularly difficult because the initiation of cracking is strongly dependent on the plastic zone and the compressive residual stresses at the crack tip.

With regard to the difference between the two main mechanisms of EAC in aqueous environments (HAC and LAD), Figure 8 shows a schematic drawing of the compressive residual stresses in the vicinity of the crack tip, to explain HAC and LAD behaviour, as well as the threshold levels. LAD is more susceptible than HAC to the effect of compressive prestressing of the crack tip by residual stresses generated during pre-cracking. This conclusion is valid for both SSRT and CST. The explanation lies in the specific localized character of LAD, which makes this phenomenon strongly dependent on compressive residual stress level *precisely* at the crack tip (*single point*). Conversely, HAC does not have so local a nature, since hydrogen diffuses towards the inner points, and the fracture phenomenon is extended over a *process zone or fracture region* (small, but not null) in the vicinity of the crack tip.

A final idea concerning stress corrosion testing. The maximum stress intensity factor during the last stage of fatigue pre-cracking must be specified by the Standards as precisely as possible, since it dramatically affects the experimental results. The present requirement ($K_{max} < K_{IEAC}$) is automatically achieved, but it is not enough to guarantee experimental results independent of the fatigue pre-cracking load, as is demonstrated throughout this paper.

CONCLUSIONS

1. The influence of the pre-cracking procedure on SSRT and CST with pre-cracked samples was shown. The experimental scatter is too high when samples are pre-cracked under different fatigue loads.
2. The concept of stress intensity threshold in environmentally assisted cracking has no intrinsic character, but is affected by the maximum stress intensity factor during fatigue pre-cracking of the samples.
3. The maximum stress intensity factor during the final stage of fatigue pre-cracking is *always* below the actual stress corrosion cracking threshold. The requirement of the ISO 7539-6 Standard is thus automatically achieved .

4. SSRT in cathodic regime (HAC) should be performed at the minimum possible strain rate. Otherwise, the effect of compressive residual stresses generated during pre-cracking must be taken into account.
5. CST and threshold measurement are particularly difficult because the initiation of cracking is strongly dependent on the plastic zone and the compressive residual stresses at the crack tip.
6. LAD is more susceptible than HAC to the effect of compressive prestressing of the crack tip by residual stresses generated during pre-cracking. This conclusion is valid for both SSRT and CST.
7. The maximum stress intensity factor during the last stage of fatigue pre-cracking must be specified by the Standards as precisely as possible, since it dramatically affects the experimental results.

ACKNOWLEDGEMENTS

The authors gratefully acknowledge the insights provided by Professor M. Elices, Head of the Material Science Department of the Polytechnical University of Madrid, during many hours of helpful discussions.

REFERENCES

(1) Parkins, R.N., ASTM STP 1210, 1993, pp. 7-21.

(2) Beavers, J.A. and Koch, G.H., ASTM STP 1210, 1993, pp. 22-39.

(3) Kane, R.D. and Wilhelm, S.M., ASTM STP 1210, 1993, pp. 40-47.

(4) ISO 7539-7: "Slow strain rate testing", 1989.

(5) ISO 7539-6: "Preparation and use of pre-cracked specimens", 1989.

(6) Lancha, A.M. and Elices, M., "Failure Analysis-Theory and Practice - ECF7", 1988, pp. 961-968.

(7) Judy, R.W., Jr., King, W.E., Jr., Hauser, J.A. and Crooker, T.W., ASTM STP 1049, 1990, pp. 410-422.

(8) Elices, M., "Fracture Mechanics of Concrete", ed. G.C. Sih, Martinus Nijhoff, Dordrecht, 1985, pp. 226-271.

(9) Astiz, M.A., Int. J. Fracture, Vol. 31, 1986, pp. 105-124, 1986.

(10) Lancha, A.M., Ph. D. Thesis, Complutense University of Madrid, 1987.

(11) Parkins, R.N., Elices, M., Sánchez Gálvez, V. and Caballero, L., Corros. Sci., Vol.22, 1982, pp. 379-405.

(12) Astafjev, V.I. and Kasatkin, E.B., "Reliability and Structural Integrity of Advanced Materials -ECF9", 1992, pp. 513-519.

(13) Rice, J.R., ASTM STP 415, 1967, pp.247-309.

(14) Toribio, J., Lancha, A.M. and Elices, M., "Reliability and Structural Integrity of Advanced Materials -ECF9", 1992, pp. 529-534.

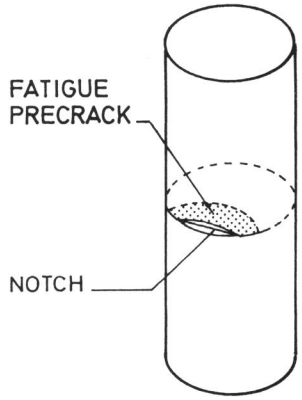

Figure 1. Pre-cracked specimen for SSRT.

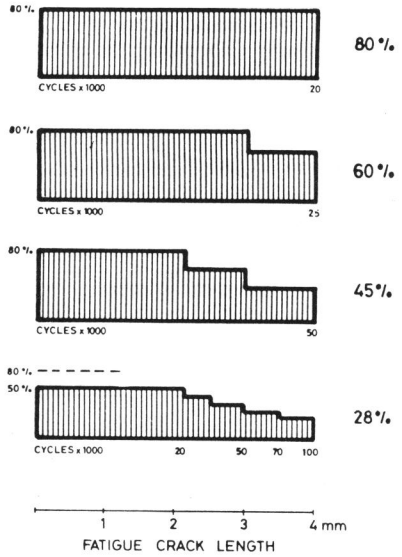

Figure 2. Fatigue pre-cracking series previous to SSRT (values in $\%K_{IC}$).

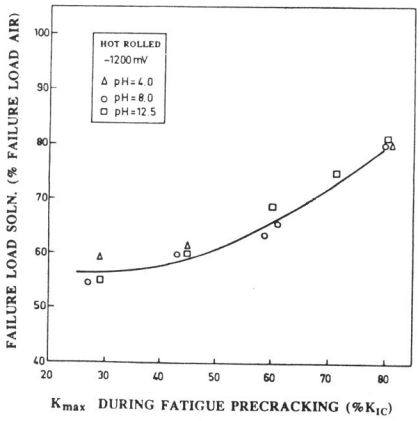

Figure 3. Results of SSRT (cathodic regime: HAC).

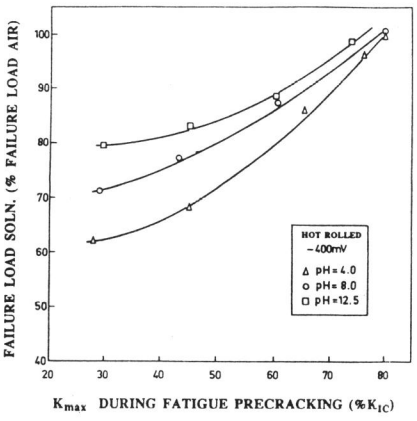

Figure 4. Results of SSRT (anodic regime: LAD).

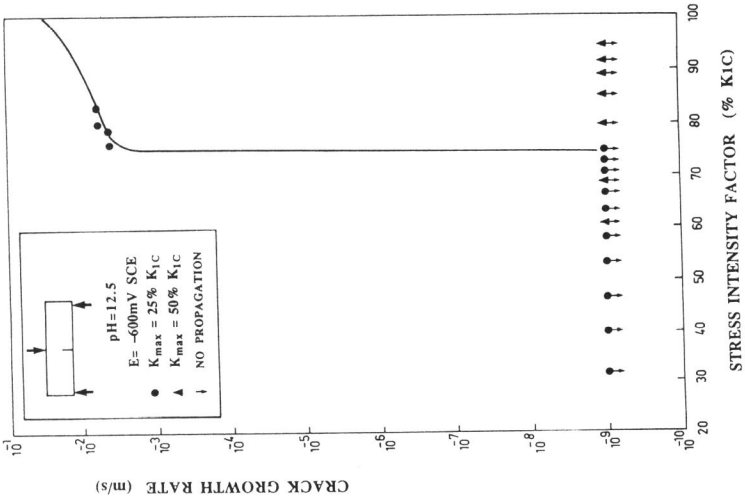

Figure 6. Results of CST (anodic regime: LAD).

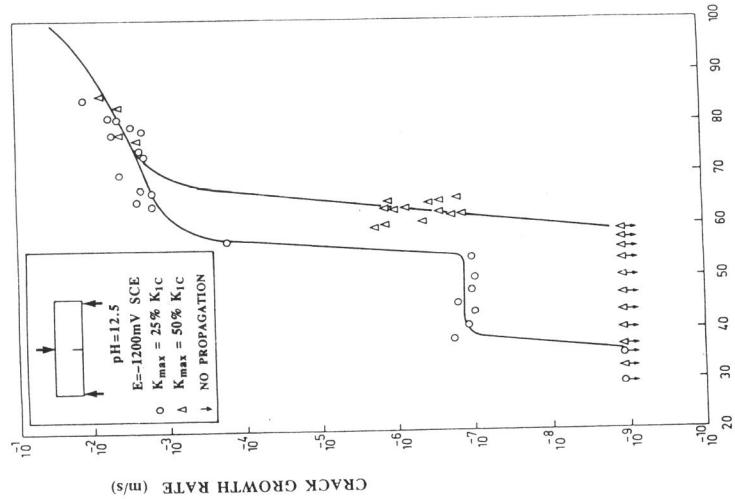

Figure 5. Results of CST (cathodic regime: HAC).

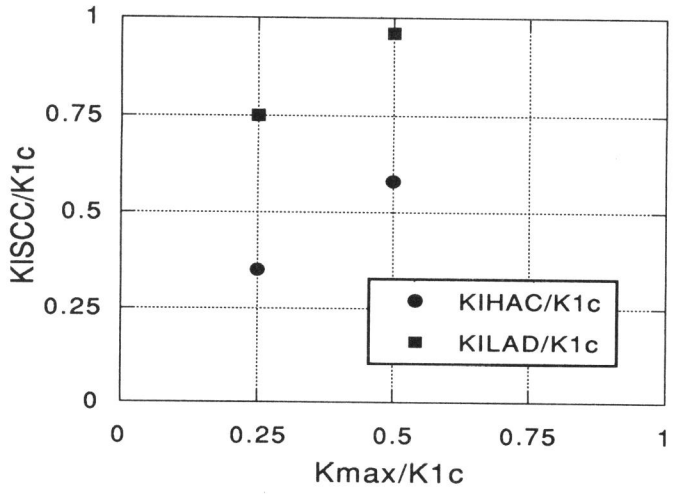

Figure 7. Threshold values plotted versus maximum stress intensity factor during fatigue pre-cracking.

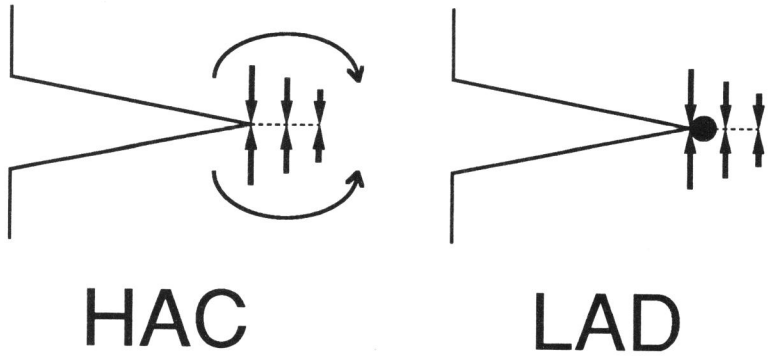

Figure 8. Schematic drawing showing plastic zone and compressive residual stresses to explain HAC and LAD behaviour, as well as threshold levels.